Shear-induced effects on critical concentration fluctuations

D. Beysens and M. Gbadamassi

Commissariat a l'Energie Atomique, Division de la Physique, Service de Physique du Solide et de Resonance Magnetique, Centre d'Etudes Nucléaire de Saclay, Boîte Postale N° 2, 91190 Gif-sur-Yvette, France

(Received 8 January 1980)

The effect of a shear flow on the critical behavior of a binary fluid (cyclohexane-aniline) has been investigated by light-scattering techniques. Turbidity and scattered-light-intensity measurements have been made, and the influence of all the independent parameters of the phenomenon were considered, i.e., temperature T, shear rate S, transfer wave vector $|\vec{q}|$, and its projection q_x along the flow direction X. The data support the Onuki-Kawasaki (OK) description, namely, (i) an effect exists only in the region $S\tau > 1$, with τ the lifetime of concentration fluctuation. (ii) The critical temperature T_c is lowered by the shear, so that $T_c = T_c(S) = T_c(0) - T_0 S^{\sigma_0}$, with $\sigma_0 = 1/3\nu$ and $\nu = 0.630$ the standard exponent of the correlation length in fluids. We find experimentally $T_0 = (1.8 \pm 0.2) \times 10^{-4}$ and $\sigma_0 = 0.53 \pm 0.03$, to be compared with the OK values 1.28×10^{-4} and 0.529. (iii) The susceptibiltiy $\chi_{\vec{q}}$ shows an anisotropy versus X, and follows a mean-field behavior versus temperature. The OK dependence $\chi_{\vec{q}}^{-1} \propto AS^{\sigma_1}[T - T_c(S)]^{\gamma} + BS^{\sigma_2} q_x^{\omega} + q^2$ fits the data well, with $\sigma_1 \simeq 0.14 \pm 0.05$ [OK: $(2\nu - 1)/3\nu = 0.137$], $\gamma \simeq 1.00 \pm 0.06$ (OK: $\gamma \neq 1$), $\omega \simeq 0.40 \pm 0.05$ (OK: 2/5), except for σ_2, whose experimental value $\sigma_2 \simeq 1 \pm 0.15$ is about twice the OK value 8/15. Discrepancies of about a factor 2 are also found for the amplitudes A and B.

I. INTRODUCTION

Recently it has been both experimentally[1] and theoretically[2] discovered that critical fluctuations from a fluid could be strongly affected by small disturbances, such as shear flow. For obvious experimental reasons (infinite compressibility of pure fluids at T_c) only binary fluids near the liquid-liquid critical point (temperature T_c) were investigated. The order parameter in this case is the difference $c - c_c$ between the concentration c of one component and its critical value c_c. The concentration fluctuations increase near T_c, and the correlation length ξ and the osmotic susceptibility $\chi = (\partial c/\partial \mu)_{p,T}$ diverge. $\mu = \mu_1 - \mu_2$ is the difference between the chemical potential μ_1, μ_2 of the components, p is pressure, T is the absolute temperature. The lifetime τ of the fluctuations correspondingly increases and diverges at T_c.

We can intuitively predict the main characteristics of the effect of shear on these concentration fluctuations. With S the shear rate ($\sec^{-1}$):

(i) The effects will only be present in the region $S\tau > 1$. Indeed, only when the lifetime τ is longer than the typical time (S^{-1}) associated with shear will the fluctuations be able to "feel" the shear. A crossover is therefore expected to occur in the region $S\tau \simeq 1$, from a standard behavior ($S\tau < 1$) to a new behavior ($S\tau > 1$).

(ii) In the direction perpendicular to the flow, the correlations will tend to be suppressed by the shear. This means that the correlation volume is no longer isotropic, leading to an anisotropy in the susceptibility.

(iii) This reduction of the correlation extent is connected to a change in the critical temperature. If $T_c(0)$ is the point where the fluctuations size diverges without shear, the effect of shear when $T = T_c(0)$ would prevent the correlation length from being infinite. The system would thus remain at a finite distance $T - T_c(S)$ from the new critical temperature $T_c(S)$.

These phenomenological predictions have been already verified by light-scattering techniques,[1] together with a less straightforward deduction concerning the effect of anisotropy which leads, as in dipolar ferromagnetics,[3] to a crossover in the region $S\tau \simeq 1$ from a standard susceptibility behavior [$\chi_q \propto (T - T_c)^{-1.24}$, $S\tau < 1$] to a mean-field behavior [$\chi_q \sim (T - T_c)^{-1}$, $S\tau > 1$]. Also, the fact that the susceptibility and thus the scattered light intensity varied with shear was used to obtain an instantaneous mapping of the shear distribution for any geometrical configuration of the flow.[4]

From a theoretical point of view, Onuki and Kawasaki (OK) have derived nearly identical general conclusions, using a renormalization-group approach. More precisely, they predicted:

(i) An effect visible in the region $S\tau > 1$. This leads to the temperature condition $T < T_s$, with

$$T_s = T_c[1 + (5\pi\eta\xi_0^3/kT_c)^{1/3\nu} S^{1/3\nu}]. \quad (1)$$

Here ξ_0 is the amplitude of the correlation length $\xi = \xi_0[(T - T_c)/T_c]^{-\nu}$ with $\nu \simeq 0.630$,[5] η is the shear visocity of the system, and k the Boltzmann constant. The expression used for the fluctuation lifetime was

$$\tau = 5\pi\eta\xi^3/kT.$$

(ii) A lowering of the critical temperature

$$T_c(S) - T_c(0) \simeq \tfrac{1}{12}[T_c(0) - T_s]. \quad (2)$$

(iii) An anisotropy with respect to the flow direction (X axis) of the susceptibility $\chi_{\vec{q}}$ in the q space, which would follow a mean-field behavior versus $T - T_c(S)$:

$$\chi_{\vec{q}}^{-1} = AS^{(2\nu-1)/3\nu}\{[T - T_c(S)]/T_c\}^{\gamma'} + BS^{8/15}|q_x|^{2/5} + q^2, \quad (3)$$

where $\gamma' = 1$, $A = (5\pi\eta/kT_c)^{(2\nu-1)/3\nu}\,\xi_0^{-1/\nu}$, and $B = (5\pi\eta/kT_c)^{8/15}$.

In the following sections we will present light-scattering experiments carried out in a critical mixture submitted to shear rates ranging from 0 to 1000 sec.$^{-1}$. We investigated both the transmission coefficient $\mathcal{T}$ of the light through the sample, connected to the integrated susceptibility $l_N\mathcal{T} \simeq \simeq -\int \chi_{\vec{q}} \cdot d\vec{q}$, and the scattered-light intensity $I_{\vec{q}} = \chi_{\vec{q}}$, versus the four independent parameters of the phenomenon: temperature T, shear S, modulus of the transfer wave vector $|\vec{q}|$, and the component q_x along the flow direction.

II. EXPERIMENTAL

The binary mixture used was the well-known cyclohexane-aniline system. Aniline was purified by fractioned distillation; cyclohexane was of spectroscopic grade. The experimental mass fraction of aniline $C = 0.4700 \pm 4 \times 10^{-4}$ was close to the critical composition (47% in weight).[6] The mixture was frozen in a special glass cell [Fig. 1(a)] which was sealed under vacuum.

The shear flow is produced in a rectangular quartz pipe C as shown in Fig. 1(b), whose dimensions in Cartesian axes $OXYZ$ are $L_X = L = 15$ cm, $a_Y = a = 0.3$ cm, $b_Z = b = 0.5$ cm. O is the center of symmetry and OY the vertical direction. This pipe C is set horizontal and, during the run, the liquid flowed along the X axis through C from a graduated cylindrical reservoir A (with a maximum fluid height difference $H_0 = 7.0$ cm) into another reservoir B.

At the end of the run some liquid remained in C so that all experiments performed with or without shear could be directly compared under exactly the same geometrical and temperature conditions. The cell was fixed on a wheel which could rotate, enabling the vessel A to be refilled at the end of the run. A mechanical locking system ensured that the pipe C returned to the same position for each run. A tube with a valve served to refill A while an extra tube served to equalize the pressures when flow took place from A to B or from B to A. This precaution was found to be necessary, as initial experiments

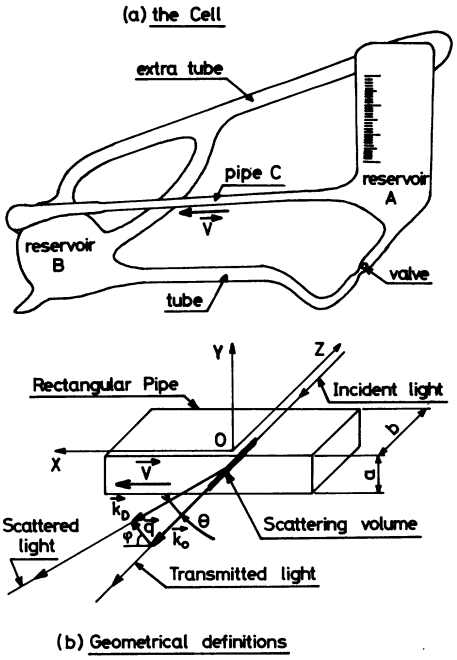

FIG. 1. (a) Cell used to produce the flow. The cell can rotate around the center of C in the plane of A and B (see text). (b) Scattering geometry. O is the center of symmetry of the pipe.

carried out without this extra tube showed anomalous phenomena due to temperature variations associated with adiabatic pressure variations.

The whole apparatus was immersed in a large water bath where it could be seen through a double window. The thermal stabilization was $\pm 2 \times 10^{-4}$ °C over more than one hour, as verified by a quartz thermometer. A laser beam ($\lambda_0 = 6328$ Å, diameter $\phi_0 = 0.35$ mm) directed parallel to the horizonal Z axis enters the pipe C at $X = 0$, $Y = Y_0 = 0.1$ cm, $Z = -0.25$ cm, as verified by a cathetometer. A lens centered on the beam images the scattering volume on the photomultiplier pinhole. The lens supports an off-center pinhole, providing a choice of scattering angle $\theta = (\vec{K}_D, \vec{K}_0)$, where $\vec{K}_0$ is the incident-light wave vector (OZ) and $\vec{K}_D$ is the scattering wave vector. When rotating the pinhole around the laser beam, θ or $|\vec{q} = \vec{K}_D - \vec{K}_0|$ remains constant while the azimuthal angle $\varphi = (\vec{q}, \vec{V})$ varies [see Fig. 1(b)]. Here $\vec{V}$ is the flow velocity vector, parallel to OX. We experimentally checked that for small scattering angles as considered the (vertical) polarization of the laser beam does not modify the scattered intensity distribution which remains isotropic in the XY plane.

In order to determine the velocity V, we used three methods:

1. *Measurement of the time variation of the*

liquid volume in A. For this, we recorded the liquid height H in A versus time t after the start of the run (Fig. 2). The following variation was found: $H = H_0 \exp(-t/t_0^{(1)})$ with $H_0 = 7.0$ cm and $t_0^{(1)} = 13.1$ sec. We thus deduced the mean velocity $\bar{V}$ in C, the ratio S_A/S_C of the cross-section area of A and C being known ($S_A/S_C = 128$): $\bar{V}_{(1)} = \bar{V}_{(1)}^0 \exp(-t/t_0^{(1)})$ with $V_{(1)}^0 = (H_0/t_0^{(1)})(S_A/S_C) \simeq 68$ cm/sec.

2. A calculation using a Poiseuille velocity distribution. For simplification, we assumed that the actual mean velocity was not too far from the mean velocity $\bar{V}_{(2)}$ in a cylindrical pipe of diameter $\phi \sim 0.4$ cm. For a liquid with density $\rho = 0.87$ g cm^{-3},[6] with viscosity $\eta \simeq 1.8\,c$P (Ref. 7) flowing in a capillary of length $L_x = 15$ cm, $\bar{V}_{(2)} = \bar{V}_{(2)}^0 \times \exp(-t/t_0^{(2)})$, with $\bar{V}_{(2)}^0 = \rho g \phi^2 H_0/32\,\eta L_x \simeq 110$ cm/sec. The exponential variation is due to the proportionality which exists between the velocity and the volume variation of liquid:

$$S_C \bar{V}_{(2)} = S_A \frac{dH}{dt} \Rightarrow H(t) = H_0 \exp\left(-\frac{t}{t_0^{(2)}}\right)$$

with $t_0^{(2)} = (S_A/S_C)\,32\,L_x\eta/\rho g\phi^2 \simeq 8.0$ sec. This value is of the same order of magnitude as the experimental value $t_0^{(1)} = 13.1$ sec.

3. A laser Doppler velocimetry determination at the precise point where the measurements are to be performed. The Doppler effect, which is related to the mean velocity of the fluctuations, gives rise to a broad spectrum when the light scattered from the volume at $Y = Y_0 = 0.1$ cm is detected in the X direction. The linewidth of this homodyne spectrum is related to the mean velocity $V_{(3)}$ of the flow at this point. In fact, a well-defined cutoff frequency is present, which allows $V_{(3)}$ to be easily determined. Figure 2 shows that

$$V_{(3)}(t, Y_0) = V_{(3)}^0(Y_0) \exp(-t/t_0^{(3)})$$

with $V_{(3)}^0(Y_0) = 93$ cm/sec and $t_0^{(3)} = t_0^{(1)} = 13.1$ sec. Assuming a Poiseuille parabolalike velocity distribution, the mean velocity in the pipe can be estimated to $\bar{V}_{(3)}^0 = V_{(3)}^0(Y_0)/2[1 - (2Y_0/a)^2 = 84$ cm/sec. The estimations of $\bar{V}_0^{(1)}$ (68 cm/sec) and $\bar{V}_0^{(2)}$ (110 cm/sec) are not very far from this experimental determination.

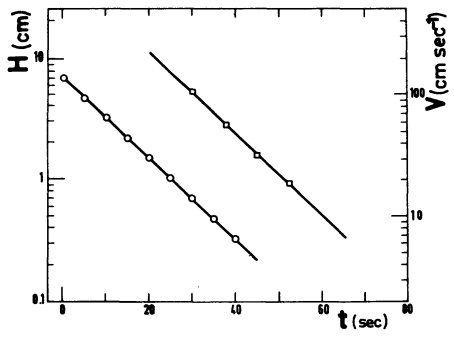

FIG. 2. Time variation of the liquid height H in A and of the mean velocity $\bar{V}$ at the measurement point (semi-log plot).

We then infer the Reynolds number $\mathcal{R}(t) = aV_{(3)}(t, Y_0)/\nu_0$ where $\nu_0 = \eta/\rho \simeq 2 \times 10^{-2}$ stokes[7] is the kinematic viscosity. The maximum value $\mathcal{R}(0) \simeq 1400$ shows that turbulence is never reached. Nevertheless, we verified that all experiments which were started at various values of $\mathcal{R}(0)$ (i.e., various heights in A) gave equivalent results.

The length l at which the parabolic velocity distribution is obtained within 1% is $l(t) = 0.03a\mathcal{R}(t) \simeq 13 \exp(-t/t_0)$ cm. At any time $t > 5$ sec the Poiseuille distribution is therefore established in the measurement region. Therefore the velocity at the measurement point can be approximated by

$$V(X, Y, Z, t) \simeq V(t, Y_0) = 2\bar{V}_0[1 - (2Y_0/a)^2]\,e^{-t/t_0}.$$

Here the influence of the velocity gradient parallel to OZ has been neglected. In fact, the corresponding gradients are smaller [ratio $(b/a)^2 \simeq 3$], and are not well defined since they are integrated over all the scattering volume. Moreover, the influence of this particular velocity gradient can be suppressed when imaging only the center of the scattering volume.

The shear at $Y = Y_0$ can therefore be deduced

$$S(Y_0 \pm \tfrac{1}{2}\phi_0, t) = \frac{dV}{dY}(Y_0 \pm \tfrac{1}{2}\phi_0, t) = (1600 \pm 280)\,e^{-t/t_0}.$$

The calculated uncertainty is due to the finite diameter ϕ_0 of the laser beam in the direction Y, as verified in Ref. 4 where the mapping of the shear was performed.

The lifetime of the concentration fluctuations in real space, i.e., at $q\xi \sim 1$ and without shear is $\tau = E(T - T_c)^{-3\nu}$ where $\nu = 0.63$ and $E = 5\pi\eta\,\xi_0^3\,T_c^{3\nu}/kT^{8,9} = 4.8 \times 10^{-6}$ cgs using the values $\xi_0 = 2.45$ Å,[10] $T_c = 303$ K, and $\eta = 1.78$ cP.[7] For experimental values $T - T_c > 1 \times 10^{-3}$ C, then $\tau < 2.2$ sec. In these time intervals the velocity distribution varies by less than a few percent in C.

The extra heating due to the shear flow can be estimated as follows: The power dissipated in a volume element is proportional to S^2 through the viscosity. With C_p the specific heat,

$$C_p \frac{\Delta T}{\Delta t} = \eta S^2.$$

During the run, the spurious heating occurs over the length $\frac{1}{2} L_x$, i.e., during the time $\Delta t = L_x/$

$2V(t, Y_0) \simeq 8L_x/S$. For time intervals lower than the thermal diffusivity time $a^2/D \sim 100$ sec ($D \sim 10^{-3}$ cm^2 sec^{-1} in liquids is the thermal diffusivity coefficient) the heat has not enough time to diffuse, and the adiabatic temperature increase can be evaluated as

$$\Delta T \simeq 8\eta L_x S/C_p .$$

Thus ΔT is proportional to S. Measurements were performed for $t > 5$ sec, or $S < 900$ sec^{-1}. In liquids, $C_p \sim 4 \times 10^7$ erg, and therefore $\Delta T < 5.10^{-5}$ K, and it is completely negligible.

The contribution of multiple scattering[11] is also negligible, considering the small dimensions of the capillary tube. This has been verified by looking at the illuminated volume, and checking that light scattered from outside the volume remains negligible. Finally, the gravitationally induced gradients do not have enough time to take place,[12] and are thus also negligible.

III. RESULTS

The experimental results are concerned with the following points:

1. The critical temperature change $T_c = T_c(S)$.
2. The crossover temperature $T_s = T_s(S)$.
3. The variation of the susceptibility $\chi_{\vec{q}}$ vs q_x at two different constant values of the modulus $|\vec{q}|$ and for various shears.
4. The variation of $\chi_{\vec{q}}$ vs $|q|$ for various shears.
5. The variation of χ_{q_X} vs T and S for two different constant values of the modulus $|\vec{q}|$.

The variation of the susceptibility in the shear direction (Y) is not reported here, owing chiefly to the lack of accuracy. Experiments are in progress concerning this point. The transmitted light intensity was used chiefly for studying point 1 and the scattered-light intensity $I_{\vec{q}}$ for points 2 to 5.

1. T_c change. The critical temperature can be defined as the temperature at which $\chi_{\vec{q}}$ diverges, i.e., τ vanishes. In Fig. 3 are reported the experimental variations of τ versus shear rate S at various temperatures. Different behaviors summarized in this Fig. 3 have been evidenced:

(a) The introduction of shear has no influence for $T > T_S(S_M)$, which is the crossover temperature T_S corresponding to the maximum shear S_M.

(b) When $T < T_S(S_M)$, the shear is seen to increase the transmission and therefore to lower the susceptibility. This suggests that the critical temperature could be a function of shear, $T_c = T_c(S)$.

(c) When $T = T_c(0)$ (the critical temperature at equilibrium) τ goes asymptotically to zero.

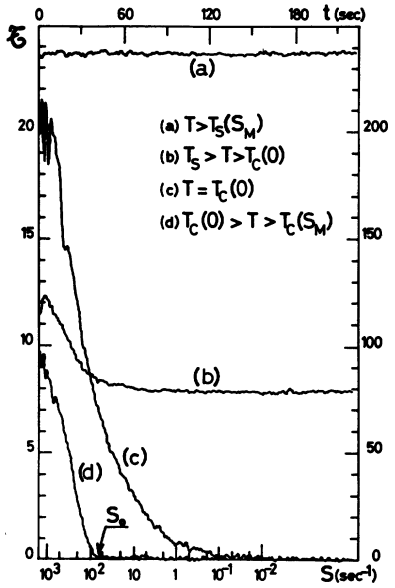

FIG. 3. Behavior of the transmitted intensity (arbitrary units) versus shear S or time $t \propto - t_0 \ln (S/S_M)$ at different temperatures (see text). The right-hand scale corresponds to (a), (b) and the left-hand scale to (c), (d).

(d) When $T_c(0) > T > T_c(S_M)$, i.e., when the run is started at a temperature slightly lower than $T_c(0)$, the transmission behaves as in (b), i.e., as in the one-phase region. A new critical temperature $T_c(S)$ is thus evidenced. The transmission goes to zero for the shear S_0, revealing the critical temperature under shear S_0: $T = T_c(S_0) = T_c(0) - \Delta T_c(S_0)$. We noticed that the scattered-light intensity diverged for the same temperature T at the same shear S_0, with $\chi_{q_Y} \gg \chi_{q_X}$, indicating that the first stage of the phase-separating process could occur in stripes parallel to the flow velocity. This is an interesting phenomenon, in accordance with the OK predictions,[2] and which we intend to study more carefully.

From Fig. 3 we can infer the variations of τ vs $T - T_c(0)$ at various shears (Fig. 4). A striking feature is that a mere change in T_c is sufficient to reduce all the data on the single equilibrium curve, i.e., $\tau[T - T_c(0), S] \simeq \tau[T - T_c(S), 0]$. This allows the variation of $\Delta T_c(S) = T_c(0) - T_c(S)$ to be evidenced.

In Fig. 5 are reported the variations of the change in T_c with S, evaluted in two different ways, first from Fig. 4 as we have just noted, and second from Fig. 3(d) using $T_c(S_0)$. A close agreement exists between these two kinds of determinations. The simple power law

$$\Delta T_c(S) = T_0 S^{\sigma_0}$$

is seen to hold, with

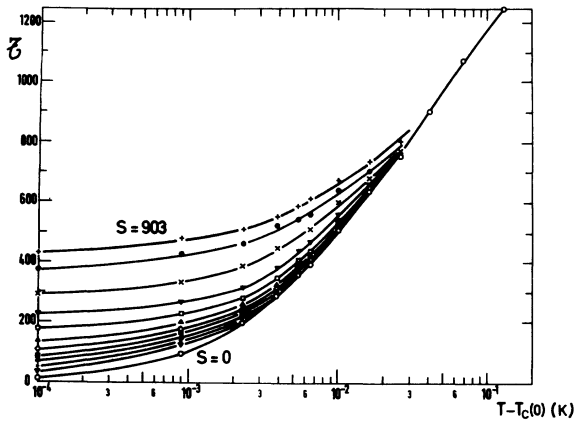

FIG. 4. Transmitted intensity (arbitrary units) versus $T - T_c(0)$ at decreasing shear rates $S = 903$, 510, 288, 163, 92, 52, 29, 16, 9.5, 5, 3, 0 sec^{-1}.

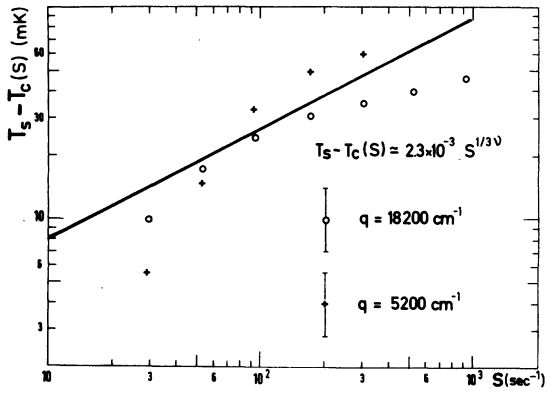

FIG. 6. Crossover temperature variation with shear S, from the scattered intensity data of Figs. 10 and 11. The straight line corresponds to a power law with an imposed exponent $\frac{1}{3}\nu = 0.53$.

$$T_0 = (1.8 \pm 0.2) \times 10^{-4} \text{ cgs}$$

and

$$\sigma_0 = 0.53 \pm 0.03.$$

These experimental values have to be compared to the OK calculation [formulas (1) and (2)]: $\sigma_0 = \frac{1}{3}\nu = 0.529$ and $(T_0)_{OK} = \frac{1}{12} T_c (5\pi\eta\, \xi_0^3/kT_c)^{1/3\nu} = 1.28 \times 10^{-4}$ cgs, using the numerical values of Sec. II. The agreement between these two sets of values is quite good.

2. The crossover temperature. In order to determine the temperature T_S below which the shear affects the fluctuations, it was found to be more reliable to use the scattered-intensity data (Figs. 10, 11) rather than the transmission data of Fig. 3. In these figures, the change of behavior is clearly evidenced and two scattering angles (wave vectors $q = 18\,200$ and 5200 cm^{-1}) were investigated.

The corresponding variation $\Delta T_S(S) = T_S(S) - T_c(S)$ is reported versus S in Fig. 6. Large uncertainties related to the crossover phenomenon itself prevents any convincing determination of amplitudes or exponents being made. Nevertheless, assuming the OK variation $T_S(S) = 13\ T_0\ S^{1/3\nu}$ and fitting the data with the imposed value $\frac{1}{3}\nu = 0.529$, we found $T_0 \simeq 1.8 \times 10^{-4}$ to be compared with 1.8×10^{-4} experimentally found with the T_c change, and 1.28×10^{-4} from OK. The agreement is remarkably good with the determination of T_0 from $T_c(S)$.

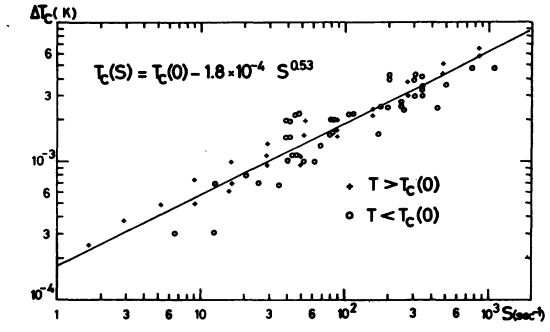

FIG. 5. Critical temperature change versus shear S. + From the variation of the transmission above $T_c(0)$ (Fig. 4); ○ from the determination of S below $T_c(0)$ (Fig. 3).

3. Susceptibility anisotropy with respect to the flow direction: $\chi_{\vec{q}}(\vec{q}_x/|\vec{q}|)$. Besides the T_c change, the most striking feature of the shear-induced effect is the anisotropy of the scattered light, and therefore of the susceptibility with respect to the flow direction. Figure 7 shows that the susceptibility is decreased in the direction X, revealing

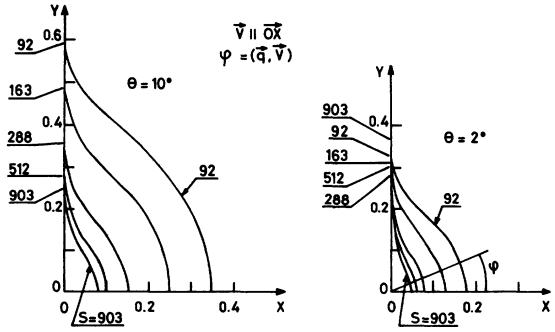

FIG. 7. Reduced scattered intensity $\chi_q(T, S)/\chi_q(T, 0)$ in the XY plane at $T - T_c(0) = 1.5$ mK (compensated from the transmission), and at two scattering angles $\theta = 2°$ and $10°$ ($q = 5200$ and $26\,000$ cm^{-1}). Polar coordinates have been used. Shear rates were $S = 903$, 512, 288, 163, and 92 sec^{-1}. The best fits to experimental data were used (see Tables I and II) with the exponent X_3 imposed at the OK value $\frac{2}{5}$

a considerable reduction of the correlation length in the shear direction Y. We notice that the effect increases with increasing shear and decreasing scattering wave vector.

Two scattering angles were carefully investigated, with a good angular resolution: $\theta_1 = 10° \pm 2$ min 30 sec and $\theta_2 = 2° \pm 12$ min, corresponding to $q_1 = 26\,000 \pm 100$ cm^{-1} and $q_2 = 5200 \pm 500$ cm^{-1}.

We will write $\Delta T(0) = T - T_c(0)$.

The anisotropy in formula (3) is determined by the q variation of the 2nd term. Two numerical calculations can be made, first by simply substituting the numerical values in (3) (OK), or second, by taking into account the results (i.e., T_0) of the transmission data (OK expt). With $\varphi = (\vec{q}, \vec{V})$, this gives:

$$\chi_q^{-1} = X_1 + X_2 |\cos\varphi|^{X_3} ,$$

$$q_1 = 26\,000 \text{ cm}^{-1} : X_1 \text{ (OK)} = 2.28 \times 10^{11} S^{0.14} [\Delta T(0) + 1.3 \times 10^{-4} S^{0.53}] + 6.74 \times 10^8 ,$$

$$X_1 \text{ (OK expt)} = 2.53 \times 10^{11} S^{0.14} [\Delta T(0) + 1.8 \times 10^{-4} S^{0.53}] + 6.74 \times 10^8 ,$$

$$X_2 \text{ (OK)} = 4.02 \times 10^8 S^{0.53} ,$$

$$X_2 \text{ (OK expt)} = 5.71 \times 10^8 S^{0.53} ,$$

$$X_3 \text{ (OK)} = X_3 \text{ (OK expt)} = \tfrac{2}{5} ;$$

$$q_2 = 5200 \text{ cm}^{-1} : X_1 \text{(OK)} = 2.28 \times 10^{11} S^{0.14} [\Delta T(0) + 1.3 \times 10^{-4} S^{0.53}] + 2.70 \times 10^7 ,$$

$$X_1 \text{ (OK expt)} = 2.53 \times 10^{11} [\Delta T(0) + 1.8 \times 10^{-4} S^{0.53}] + 2.70 \times 10^7 ,$$

$$X_2 \text{ (OK)} = 2.11 \times 10^8 S^{0.53} ,$$

$$X_2 \text{ (OK expt)} = 3.00 \times 10^8 S^{0.53} ,$$

$$X_3 \text{ (OK)} = X_3 \text{ (OK expt)} = \tfrac{2}{5} .$$

The experimental temperature difference is $\Delta T(0) = 1.5 \times 10^{-3}$ K for all data. The value X_i (OK) and X_i (OK expt) are close together, so that in Tables I and II where the values of the ratio X_2/X_1 are listed for various shears we report only the mean value

$$X_2/X_1 = \tfrac{1}{2}[(X_2/X_1)_{\text{OK expt}} + (X_2/X_1)_{\text{OK}}] \pm \tfrac{1}{2}[(X_2/X_1)_{\text{OK expt}} - (X_2/X_1)_{\text{OK}}] .$$

Also reported are the results concerning the experimental data. A program of statistical refining

TABLE I. Fit of χ_q^{-1} to $X_1 + X_2 |\cos\varphi|^{X_3}$ for $q = 5200$ cm^{-1} and $T - T_c(0) = 1.5$ mK ($\tau \simeq 1$ sec). $(X_2/X_1)_{OK}$ is the amplitude expected from the OK theory. Brackets indicate that in the fit the parameter was held constant at the quoted value.

S (sec^{-1}) or $S\tau$	X_3	X_2/X_1	$(X_2/X_1)_{OK}$	Q	$\sigma(\chi_q)$ %
903	0.36 ± 0.05		2.07 ± 0.01	0.92	28
	(0.40)			0.903	28
510	0.30 ± 0.05		2.08 ± 0.01	0.71	23
	(0.40)	12 ± 10		0.65	23
288	0.25 ± 0.04		2.05 ± 0.03	0.67	21
	(0.40)	4.8 ± 2.7		0.56	21
163	0.20 ± 0.04		1.98 ± 0.05	0.64	19
	(0.40)	2.2 ± 1.1		0.53	20
92	0.14 ± 0.04		1.88 ± 0.08	0.66	18
	(0.40)	1.1 ± 0.6		0.55	18
52	0.10 ± 0.04		1.74 ± 0.09	0.71	17
	(0.40)	0.6 ± 0.4		0.63	18
29	0.07 ± 0.03		1.56 ± 0.10	0.74	15
	(0.40)	0.3 ± 0.2		0.70	16
16	0.05 ± 0.03		1.38 ± 0.10	0.87	14
	(0.40)			0.84	14.5

TABLE II. Fit of χ_q^{-1} to $X_1 + X_2 |\cos\varphi|^{X_3}$ for $q = 26\,000$ cm^{-1} and $T - T_c(0) = 1.5$ mK ($\tau \simeq 1$ sec). $(X_2/X_1)_{OK}$ is the amplitude expected from OK theory. Brackets indicate that in the fit the parameter was held constant at the quoted value.

S (sec^{-1}) or $S\tau$	X_3	X_2/X_1	$(X_2/X_1)_{OK}$	Q	$\sigma(\chi_q)$ %
903	0.52 ± 0.12	2.8 ± 0.8	3.45 ± 0.05	0.72	12.2
	(0.40)	3.4 ± 0.7		0.69	12.2
510	0.52 ± 0.14	2.24 ± 0.6	3.3 ± 0.1	0.80	12.5
	(0.40)	2.74 ± 0.6		0.75	12.7
288	0.64 ± 0.18	1.5 ± 0.4	3.1 ± 0.1	0.996	11
	(0.40)	1.90 ± 0.35		0.87	11.5
163	0.9 ± 0.2	1.1 ± 0.2	2.8 ± 0.2	0.99	9.8
	(0.40)	1.3 ± 0.3		0.75	10.5
92	1.5 ± 0.5	1.0 ± 0.2	2.5 ± 0.2	0.96	8.7
	(0.40)	0.9 ± 0.2		0.61	9.9
52	2.0 ± 1.0	0.73 ± 0.2	2.1 ± 0.2	0.98	7.3
	(0.40)	0.54 ± 0.15		0.59	8.8
29	3.2 ± 1.6	0.65 ± 0.2	1.8 ± 0.2	0.97	6.3
	(0.40)				
16	3.8 ± 1.8	0.53 ± 0.16	1.45 ± 0.15	0.88	5.5
	(0.40)				

(M. Tournarie[13]) has been used, giving the standard error $\sigma(\chi_q)$ and a "quality coefficient" Q which measures the contribution of the statistical error to the total error. $Q = 1$ when no systematical distortions to the fit exist and Q drastically decreases if there are systematic distortions.

The data (noncorrected for the transmission) were fitted to the following variation:

$$\chi_q^{-1} = X_1 + X_2 |\cos\varphi|^{X_3} ,$$

with X_i the adjustable parameters. In a first step, all parameters were set free, so that both X_3 and X_2/X_1 could be compared to the OK values. Results are summarized in Tables I and II. In Fig. 8 are reported the log-log variations of χ_q vs $\cos\varphi$ for the various shears and the two values of q.

For X_3, we see that the experimental values are close to $\frac{2}{5}$ for the highest shears ($X_3 = 0.52 \pm 0.12$ for $S = 903$ sec^{-1}, $q = 26\,000$ cm^{-1}, $X_3 = 0.36 \pm 0.05$ for $S = 903$ sec^{-1}, $q = 5200$ cm^{-1}). When the shear decreases, X_3 increases for the higher q value ($X_3 = 3.8 \pm 1.8$, $S = 16$ sec^{-1}, $q = 26\,000$ cm^{-1}) but decreases for the lower q value ($X_3 = 0.05 \pm 0.03$, $S = 16$ sec^{-1}, $q = 5200$ cm^{-1}). The amplitude ratio X_2/X_1 is well defined only for the highest $q = 26\,000$ cm^{-1}. Its order of magnitude is correct for all shears, and agrees well with the OK value for the highest shears [$S = 903$ sec^{-1}, $X_2/X_1 = 2.8 \pm 0.8$ $(X_2/X_1)_{OK} = 3.45 \pm 0.05$].

In order to have a better determination of the amplitudes, we next impose X_3 to its OK value. The highest q, with the highest shears, gives the better agreement [$q = 26\,000$ cm^{-1}, $S = 903$ sec^{-1}, $X_2/X_1 = 3.4 \pm 0.7$, $(X_2/X_1)_{OK} = 3.45 \pm 0.05$]. In all cases the order of magnitude is correct. For the lowest q, a rather good agreement is obtained for the mean shears, the highest shears giving rise to an undetermined value [$q = 5200$ cm^{-1}, $S = 163$ sec^{-1}, $X_2/X_1 = 2.2 \pm 1.1$, $(X_2/X_1)_{OK} = 1.98 \pm 0.05$].

4. Variation of χ_{q_X} with $|\vec{q}|$. Following formula (3), the same kind of variation as in point 3 should be found when $|q|$ is varied from 3900 to 23 400 cm^{-1}. We consider the experimental data concerning the scattered intensity in the flow direction, where the influence of q is preponderant. Moreover, in this direction, the Doppler effect very efficiently filters the intensity fluctuations. Here also, the intensity data are not corrected for transmission, so that the shear variation of χ_q cannot be determined.

The (OK) and (OK expt) formulations can be written as:

$$\chi_q^{-1} = X_1 + X_2 q^{X_3} + X_4 q^2 ;$$

$$(X_1/X_4)_{OK} = 2.28 \times 10^{11} S^{0.14} [\Delta T(0) + 1.3 \times 10^{-4} S^{0.53}] ,$$

$$(X_2/X_4)_{OK\ expt} = 2.53 \times 10^{11} S^{0.14} [\Delta T(0) + 1.8 \times 10^{-4} S^{0.53}] ,$$

$$(X_2/X_4)_{OK} = 6.90 \times 10^6 S^{0.53} ,$$

$$(X_2/X_4)_{OK\ expt} = 9.79 \times 10^6 S^{0.53} ,$$

$$X_3(\mathrm{OK}) = X_3(\mathrm{OK\ expt}) = \tfrac{2}{5} .$$

The experiments were carried out at $\Delta T(0) = 3.7 \times 10^{-3}$ K and in the flow direction where $q_X = q$. The data (Fig. 9) were fitted to the same expression, where X_i are the adjustable parameters.

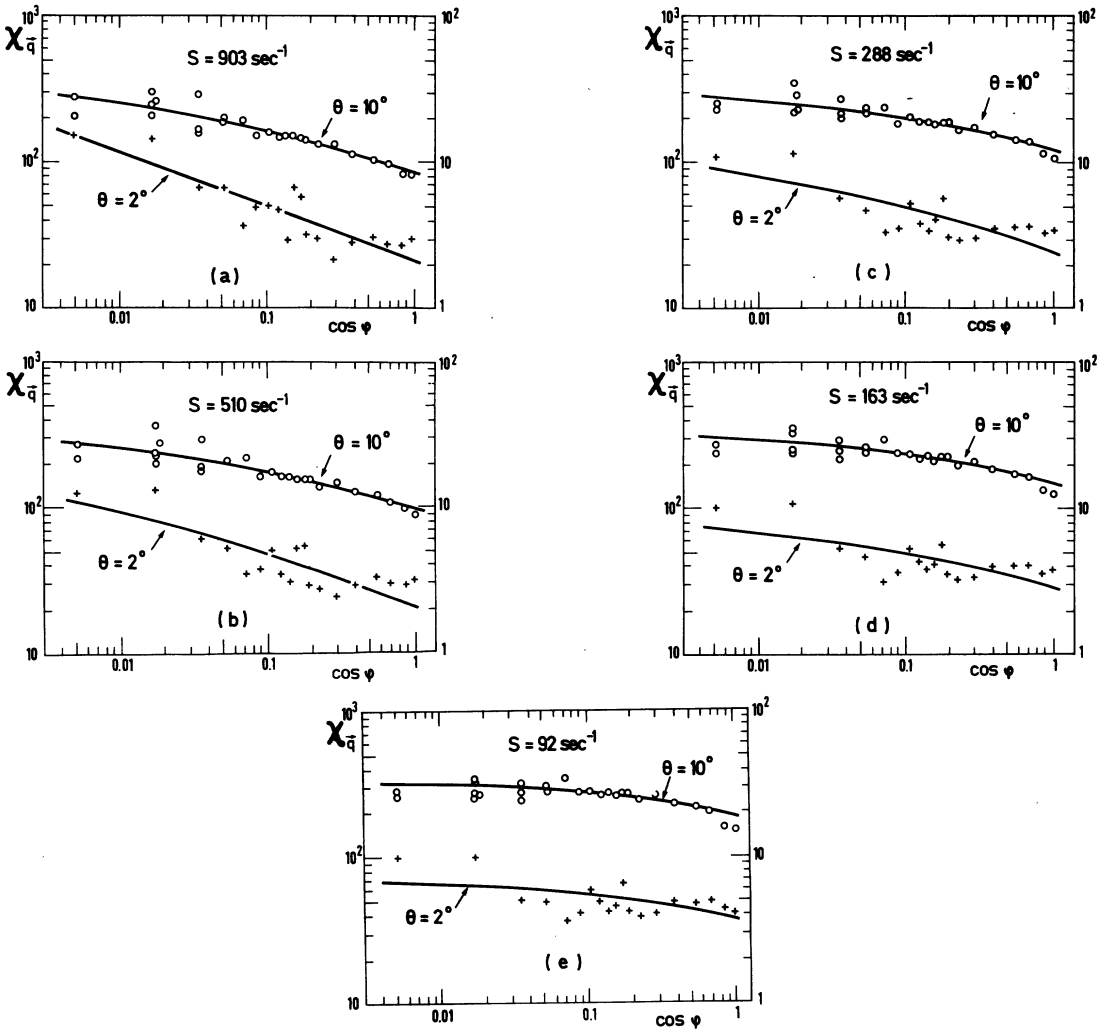

FIG. 8. (a)–(e). Scattered intensity $\chi_{\vec{q}}$ vs cos φ [$\varphi = (\vec{q}, \vec{V})$] at $T - T_c(0) = 1.5$ mK, in a log-log plot, and at the scattering angles $\theta = 10°$ ($q_2 = 26\,000$ cm^{-1}) (right-hand scale) and $\theta = 2°$ ($q_1 = 5200$ cm^{-1}) (left-hand scale). Lines correspond to the fits from Tables I and II with the exponent X_3 imposed at the OK value $\frac{2}{5}$.

TABLE III. Fit of $\chi_{q_X}^{-1}$ to $X_1 + X_2 q_X^{X_3} + X_4 q^2$ for $T - T_c(0) = 3.7$ mK and $q = q_X$ ranging from 3900 to 23 400 cm^{-1}. Parentheses indicate that in the fit the parameter X_3 was held constant at the quoted value.

S (sec^{-1})	X_1	X_2	X_3	X_4	Q	$\sigma(\chi_q)$ %
903	$(1.65 \pm 1.34) \times 10^{-2}$	$(3.1 \pm 18) \times 10^{-5}$	0.74 ± 0.6	$(1.1 \pm 42) \times 10^{-12}$	0.534	2.0
	$(2.85 \pm 2.7) \times 10^{-3}$	$(9.9 \pm 0.9) \times 10^{-4}$	(0.40)	$(2.0 \pm 0.6) \times 10^{-12}$	0.543	2.1
510	$(1.3 \pm 3.6) \times 10^{-4}$	$(1.16 \pm 0.24) \times 10^{-3}$	0.38 ± 0.02	$(2.8 \pm 8) \times 10^{-14}$	0.587	4.0
	$(1.8 \pm 2) \times 10^{-3}$	$(9.3 \pm 0.6) \times 10^{-4}$	(0.40)	$(2.7 \pm 7) \times 10^{-14}$	0.568	4.0
288	$(1.3 \pm 4.3) \times 10^{-4}$	$(1.0 \pm 0.17) \times 10^{-3}$	0.38 ± 0.018	$(2.8 \pm 10) \times 10^{-14}$	0.631	3.2
	$(1.6 \pm 1.4) \times 10^{-3}$	$(8.0 \pm 3.6) \times 10^{-4}$	(0.40)	$(2.8 \pm 8) \times 10^{-14}$	0.609	3.2
163	$(7.9 \pm 6.5) \times 10^{-3}$	$(1.6 \pm 3.2) \times 10^{-4}$	0.5 ± 0.2	$(3 \pm 11) \times 10^{-14}$	0.758	3.6
	$(3.0 \pm 2.5) \times 10^{-3}$	$(6.2 \pm 0.8) \times 10^{-4}$	(0.40)	$(1.8 \pm 5) \times 10^{-12}$	0.841	3.9
92	$(11 \pm 3.5) \times 10^{-3}$	$(3.2 \pm 6.6) \times 10^{-5}$	0.6 ± 0.2	$(3 \pm 17) \times 10^{-14}$	0.641	3.1
	$(6 \pm 2) \times 10^{-3}$	$(4.2 \pm 0.7) \times 10^{-4}$	(0.40)	$(4.3 \pm 4) \times 10^{-12}$	0.704	3.4
52	$(11 \pm 2) \times 10^{-3}$	$(8 \pm 16) \times 10^{-6}$	0.75 ± 0.2	$(3 \pm 20) \times 10^{-14}$	0.439	2.4
	$(7.7 \pm 1.7) \times 10^{-3}$	$(2.9 \pm 0.6) \times 10^{-4}$	(0.40)	$(5 \pm 3) \times 10^{-12}$	0.520	2.7
29	$(8.6 \pm 26) \times 10^{-3}$	$(3.2 \pm 53) \times 10^{-4}$	0.35 ± 1.5	$(9.6 \pm 10) \times 10^{-12}$	0.341	1.4
	$(9.5 \pm 1.3) \times 10^{-3}$	$(1.8 \pm 0.4) \times 10^{-4}$	(0.40)	$(9 \pm 2) \times 10^{-12}$	0.331	1.7

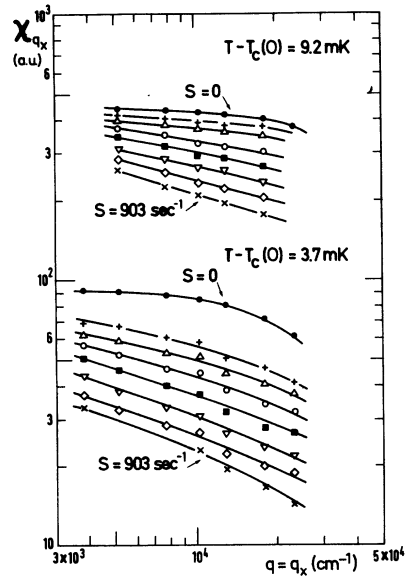

FIG. 9. Scattered intensity in the flow direction $\chi_{\vec{q}}$ vs $\vec{q}$ with $\vec{q}$ parallel to OX. Data are not corrected for the transmission. Two temperatures are reported. The analysis is made in Tables III and IV. The shear rates are: $S=0$, 29. 52, 92, 163, 288, 510, 903 $\sec^{-1}$.

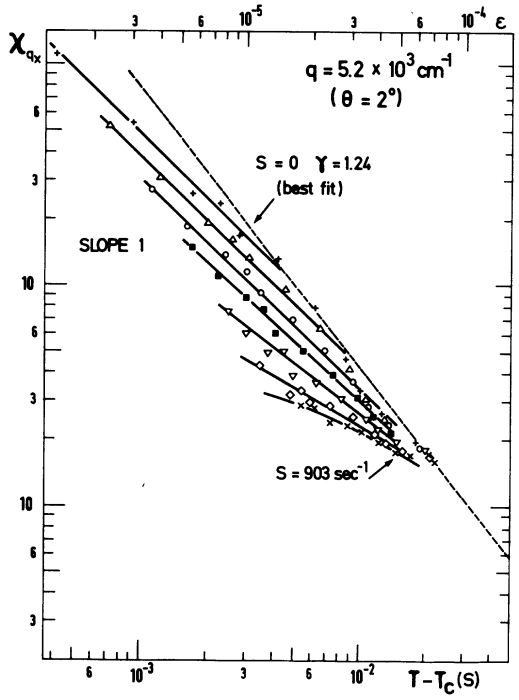

FIG. 10. Scattered intensity in the flow direction χ_{q_X} vs $T-T_c(S)$ at various shears (see caption of Fig. 9) for $q=5200$ cm^{-1}. The dotted line is the best fit to all experimental data obtained with $S=0$, and corresponds to the normal behavior $\simeq (T-T_c)^{-1.24}$. These data have been analyzed in Table V.

Table III summarizes the results. The exponent X_3 is rather well determined for shears 510 and 288 $\sec^{-1}$: $X_3 = 0.38 \pm 0.02$, to be compared to the OK value: $\frac{2}{5}$.

The other shears also gave values which are compatible with this determination, but no amplitudes could be extracted. So we fixed X_3 at the value $\frac{2}{5}$ and again fitted the results. Table IV shows that the accuracy is sufficient only for four values of shear. All the results agree with OK within the experimental errors. Here also, the mean value between OK and OK expt has been reported, the higher values corresponding to OK expt.

Other data, which are not reported here, and which concern the temperature difference $\Delta T(0) = 9.2 \times 10^{-3}$ K, support the same general conclusions, although with a lower accuracy.

TABLE IV. Amplitude ratios from Table III with X_3 imposed at the value 0.40. The values OK quoted are deduced from the Onuki-Kawasaki theory.

S	X_2/X_1 (10^{-2})	$(X_2/X_1)_{OK}$ (10^{-2})	X_2/X_4 (10^8)	$(X_2/X_4)_{OK}$ (10^8)
903			5 ± 2	3.07 ± 0.53
92	7 ± 3.5	3.71 ± 0.70	1 ± 1	0.919 ± 0.016
52	4 ± 2	2.65 ± 0.25	0.58 ± 0.46	0.677 ± 0.0117
29	2.0 ± 0.7	2.76 ± 0.25	0.20 ± 0.09	0.347 ± 0.086

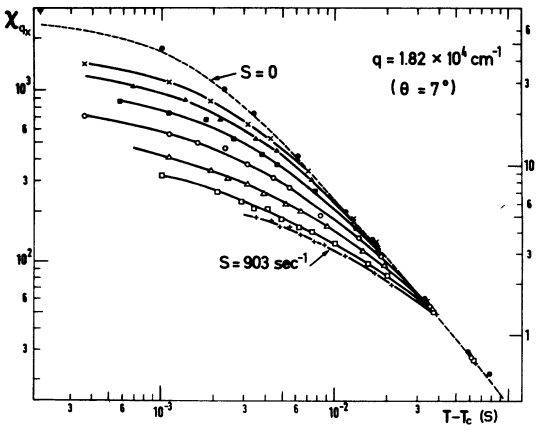

FIG. 11. Scattered intensity in the flow direction χ_{q_X} vs $T-T_c(S)$ at various shears (see caption of Fig. 9) for $q=18\,200$ cm^{-1}. The dotted line corresponds to $S=0$ and behaves as $\simeq \{\xi_0^2[(T-T_c)/T_c]^{+1.24} + q^2\}^{-1}$. These date have been analyzed in Table VI.

TABLE V. Fit of $\chi_{q_X}^{-1}$ to $X_1\,[T-T_c(S)]^{X_2}S^{X_3}+X_4S^{X_5}+X_6$ for $q_1=5200$ cm^{-1}. Brackets indicate that in the fit the parameter was held constant at the quoted value.

Determination of	X_1 (10^{-6})	X_2	X_3	X_4 (10^{-7})	X_5	X_6 (10^{-9})	Q	$\sigma(\chi_q)$ %
≃ all free	8 ± 2	1.12 ± 0.05	(0.14)	7.0 ± 5.5	1.22 ± 0.12	1.6 ± 100	0.873	8.7
	8 ± 2	1.11 ± 0.08	0.14 ± 0.05	6.8 ± 6	1.22 ± 0.13	(0)	0.874	9
exponent X_2	3.3 ± 1.7	1.3 ± 0.1	(0.14)	272 ± 56	(0.533)	1 ± 30	0.386	12
exponents X_3, X_5	9.7 ± 1.2	(1.0)	0.216 ± 0.003	2.6 ± 0.5	1.33 ± 0.04	1.3 ± 60	0.880	9.2
exponent X_5	13.1 ± 0.3	(1.0)	(0.14)	2.6 ± 0.2	1.38 ± 0.02	1 ± 40	0.845	9.8
amplitudes	15 ± 1	(1.0)	(0.14)	107 ± 45	(0.533)	0.9 ± 20	0.243	11

5. Temperature and shear variation of χ_{q_X}. The temperature dependence of the susceptibility in the flow direction has been investigated at various shears and for two values of q (scattering angles 2° and 7°). The data are corrected for the shear dependence of the transmission (Fig. 4). Figure 10 (small $q_1=5200$ cm^{-1}) clearly shows a change of behavior in the region where $T\sim T_s$, that is, χ_{q_X} varies as $[T-T_c(S)]^{-\gamma}$ with $\gamma=1.24$ the standard value in fluids when $T>T_s$, whereas it varies as $[T-T_c(S)]^{-\gamma'}$ with $\gamma'\simeq 1$ the meanfield exponent, when $T<T_s$. This is not so clear in Fig. 11 where we report χ_{q_X} for a bigger $q_2=18\,200$ cm^{-1}, due to the standard rounding off when $q\xi>1$.

We fitted the data in the region $T<T_s$ to the following OK variation [formula (3)] where X_i are the adjustable parameters:

$$\chi_{q_X}^{-1}=X_1[\Delta T_c(S)]^{X_2}S^{X_3}+X_4S^{X_5}+X_6\,.$$

The results of the fit are reported in Tables V (q_1) and VI (q_2). For both wave vectors it was quite impossible to obtain determined X_i values when all parameters were set free. So we decided to impose the exponent X_3 which is expected to be very small from OK (0.14). For the lowest wave vector q_1 used, where X_6 is expected to be very small, we also tried a fit with $X_6=0$.

The temperature-dependent exponent is seen to have the mean-field value 1.12 ± 0.05 or 1.11 ± 0.08 (q_1) and 0.984 ± 0.068 (q_2). The weak exponent X_3 is determined when $X_6=0$ is imposed, $X_3=0.14\pm0.05$ (q_1), in close agreement with the OK value; but the shear dependence exponent X_5 is found to be about twice the expected value 0.533, $X_5=1.22\pm0.12$ (q_1) and 0.84 ± 0.14 (q_2). We will discuss the amplitudes X_1, X_4, X_6 below.

We next tried to increase the accuracy of X_2 by fixing both exponents X_3 and X_5 to their OK values; but the statistical quality of these fits was not very good, showing systematic discrepancies (q_1: $Q=0.386$ with $\sigma=12\%$; q_2: $Q=0.569$ with $\sigma=6\%$), especially for q_1. So this improvement is rather delusive and the values found, 1.3 ± 0.1 (q_1) and 1.04 ± 0.04 (q_2), are not very reliable.

The next step was to fix X_2 to the mean-field value and determine both X_3 and X_5, or X_5 alone with X_3 fixed. X_3 was found to be not very far from the value predicted by OK (0.14): $X_3=0.216\pm0.003$ (q_1) and 0.23 ± 0.05 (q_2). The X_5 exponent is

TABLE VI. Fit of $\chi_{q_X}^{-1}$ to $X_1\,[T-T\,(S)]^{X_2}S^{X_3}+X_4S^{X_5}+X_6$ for $q_2=18\,200$ cm^{-1}. Brackets indicate that in the fit the parameter was held constant at the quoted value.

Determination of	X_1 (10^{-5})	X_2	X_3	X_4 (10^{-5})	X_5	X_6 (10^{-4})	Q	$\sigma(\chi_q)$ %
≃ all free	2.3 ± 0.7	0.984 ± 0.068	(0.14)	1.2 ± 1.1	0.84 ± 0.14	2.9 ± 1.3	0.872	6
exponent X_2	1.8 ± 0.3	1.04 ± 0.04	(0.14)	8.7 ± 0.4	(0.533)	$(1.5\pm90)10^{-5}$	0.569	6
exponents X_3, X_5	1.4 ± 0.4	(1.0)	0.23 ± 0.05	1.5 ± 1.5	0.80 ± 0.15	3.5 ± 1.4	0.803	5
exponent X_5	2.15 ± 0.05	(1.0)	(0.14)	1.3 ± 0.6	0.84 ± 0.08	2.9 ± 0.7	0.871	6
amplitudes	2.17 ± 0.07	(1.0)	(0.14)	8.4 ± 0.25	(0.533)	$(1.4\pm75)10^{-5}$	0.533	6

TABLE VII. Principal results concerning the temperature change $\Delta T_c(S) = T_c(S) - T_c$ and the susceptibility $\chi_q^{-1} = AS^{\sigma_1}[\Delta T_c(S)]^{\gamma} + BS^{\sigma_2} q_x^{\omega} + q^2$ (see text). Parentheses indicate the OK values.

Critical temp. change $\Delta T_c(S) = -T_0 S^{\sigma_0}$		Anisotropy term $BS^{\sigma_2} q_x^{\omega}$			Temperature term $AS^{\sigma_1}[\Delta T_c(S)]^{\gamma}$		
Exponent	Amplitude	Exponents		Amplitude	Exponents		Amplitude
σ_0 (0.529)	T_0 (1.28×10^{-4})	σ_2 (0.533)	ω (0.400)	B (6.85×10^6)	σ_1 (0.137)	γ (1.00)	A/B (1.10×10^7)
0.53 ± 0.03 [a]	$(1.8 \pm 0.2) \times 10^{-4}$ [a]	1.22 ± 0.12 [j]	0.36 ± 0.05 [b]	$(13 \pm 5) \times 10^6$ [i]	0.14 ± 0.05 [l]	1.12 ± 0.05 [n]	$(0.40 \pm 0.03) \times 10^7$ [p]
		0.84 ± 0.14 [k]	0.30 ± 0.05 [c]		0.23 ± 0.05 [m]	0.984 ± 0.068 [o]	
			0.52 ± 0.12 [d]				
			0.52 ± 0.14 [e]				
			0.64 ± 0.18 [f]				
			0.38 ± 0.02 [g]				
			0.38 ± 0.018 [h]				

[a] From transmission measurements of Sec. III, point 1.
[b] From Table I, $S = 903$ sec^{-1}, $q = 5200$ cm^{-1}.
[c] From Table I, $S = 510$ sec^{-1}, $q = 5200$ cm^{-1}.
[d] From Table II, $S = 903$ sec^{-1}, $q = 26\,000$ cm^{-1}.
[e] From Table II, $S = 510$ sec^{-1}, $q = 26\,000$ cm^{-1}.
[f] From Table II, $S = 288$ sec^{-1}, $q = 26\,000$ cm^{-1}.
[g] From Table III, $S = 510$ sec^{-1}.
[h] From Table III, $S = 288$ sec^{-1}.
[i] From Table IV, $S = 903$; $\omega = 0.40$ imposed.
[j] From Table V, all free.
[k] From Table VI, all free.
[l] From Table V, all free but $X_6 = 0$.
[m] From Table VI, X_3, X_5 imposed.
[n] From Table V, all free.
[o] From Table VI, all free.
[p] From Table VI, X_2, X_3, X_5 imposed.

again found to be larger than the OK value (0.533): $X_5 = 1.38 \pm 0.02$ (q_1) and 0.84 ± 0.08 (q_2).

For the amplitude ratios X_1/X_6, X_4/X_6, or X_4/X_1, we found only one value which is determined: $X_4/X_1 = 3.9 \pm 0.3$ (q_2, exponents X_2, X_3, X_5 imposed), which is to be compared with 1.54(OK value) and 1.94(OK expt value).

IV. CONCLUSION

In Table VII are summarized all our results concerning the transmission data and their relation to the T_c change, together with the scattered intensity data and their connection to the susceptibility behavior of the system. The influence of the wave vector of the fluctuations, the direction of flow, the amplitude of shear, and the distance to the critical temperature were investigated.

The agreement with OK theory is generally very good, especially for the T_c change, the q variation of the susceptibility and its temperature dependence, where clearly a mean-field behavior is evidenced. An exception concerns the shear variation of the anisotropy term, whose exponent is found to be high compared to the expected value.

We did not investigate in detail the susceptibility in the shear direction, owing to lack of accuracy. Experiments are in progress concerning this particular point which, when completed, will provide information concerning the dynamic of the shear-modified fluctuations through the power spectrum of the scattered light.

ACKNOWLEDGMENTS

It is a pleasure to thank P. Bergé for fruitful discussions and A. Onuki and K. Kawasaki for having communicated their preprints and for very interesting discussions.

[1] (a) D. Beysens, M. Gbadamassi, and L. Boyer, Phys. Rev. Lett. 43, 1253 (1979); (b) D. Beysens and M. Gbadamassi, J. Phys. (Paris) Lett. 40, L 565 (1979); (c) D. Beysens, in *Ordering in Strongly Fluctuating Condensed Matter Systems*, *NATO Report*, 1979, edited by T. Riste (Plenum, New York, 1980).

[2] A. Onuki and K. Kawasaki, (a) Ann. Phys. 121, 456 (1979); (b) Progr. Theor. Phys. Suppl. 64, 436 (1978); (c) Phys. Lett. A 72, 233 (1979).

[3] J. Als Nielsen and R. J. Birgeneau, Am. J. Phys. 45, 554 (1977).

[4] D. Beysens and M. Gbadamassi, Phys. Lett. 77A, 171 (1980).

[5] J. C. Le Guillou and J. Zinn-Justin, Phys. Rev. Lett. 39, 95 (1977).

[6] J. Timmermans, *Physico-Chemical Constants of Binary Systems in Concentrated Solutions* (Interscience, New York, 1953), Vol. I; D. Atack and O. K. Rice, Disc. Trans. Farad. Soc. 23, 2428 (1953).

[7] G. d'Arrigo, L. Mistura, and P. Tartaglia, J. Chem. Phys. 66, 80 (1977).

[8] K. Kawasaki, Ann. Phys. (New York) 61, 1 (1970).

[9] E. D. Siggia, B. I. Halperin, and P. C. Hohenberg, Phys. Rev. B 13, 2110 (1976).

[10] See P. Calmettes, thesis, Paris, 1978, Université P.M. Curie (unpublished); P. Calmettes, I. Lagües, and C. Laj, Phys. Rev. Lett. 28, 478 (1972); P. Calmettes and C. Laj, *ibid.* 36, 1372 (1976).

[11] See, for instance, D. Beysens and G. Zalczer, Opt. Commun. 26, 172 (1978).

[12] See, for instance, (a) S. C. Greer, T. E. Block, and C. M. Knobler, Phys. Rev. Lett. 34, 250 (1975); and (b) M. Giglio and A. Vendramini, *ibid.* 35, 168 (1975).

[13] M. Tournarie, J. Phys. (Paris) 30, 47 (1969).